4980 J. Med. Chem. 2010, 53, 4980–4988
DOI: 10.1021/jm1000198

Journal of Medicinal Chemistry Article

Fast-Forwarding Hit to Lead: Aurora and Epidermal Growth Factor Receptor Kinase Inhibitor Lead Identification†

Mohane Selvaraj Coumar,[‡,#] Chang-Ying Chu,[‡,#] Cheng-Wei Lin,[‡,§] Hui-Yi Shiao,[‡] Yun-Lung Ho,[‡] Randheer Reddy,[‡] Wen-Hsing Lin,[‡] Chun-Hwa Chen,[‡] Yi-Hui Peng,[‡] Jiun-Shyang Leou,[‡] Tzu-Wen Lien,[‡] Chin-Ting Huang,[‡] Ming-Yu Fang,[‡] Szu-Huei Wu,[‡] Jian-Sung Wu,[‡] Santhosh Kumar Chittimalla,[‡] Jen-Shin Song,[‡] John T.-A. Hsu,[‡,∥] Su-Ying Wu,[‡] Chun-Chen Liao,[§,⊥] Yu-Sheng Chao,[‡] and Hsing-Pang Hsieh*[,‡]

[‡]*Division of Biotechnology and Pharmaceutical Research, National Health Research Institutes, 35 Keyan Road, Zhunan, Miaoli County 350, Taiwan, ROC,* [§]*Department of Chemistry, National Tsing Hua University, 101 Guangfu Road Sec. 2, Hsinchu 300, Taiwan, ROC,* [∥]*Department of Biological Science and Technology, National Chiao Tung University, 1001 University Road, Hsinchu 300, Taiwan, ROC, and* [⊥]*Department of Chemistry, Chung Yuan Christian University, 200 Zhongbei Road, Zhongli 320, Taiwan, ROC.* [#] *These authors contributed equally to this work.*

Received January 7, 2010

A focused library of furanopyrimidine (350 compounds) was rapidly synthesized in parallel reactors and in situ screened for Aurora and epidermal growth factor receptor (EGFR) kinase activity, leading to the identification of some interesting hits. On the basis of structural biology observations, the hit **1a** was modified to better fit the back pocket, producing the potent Aurora inhibitor **3** with submicromolar antiproliferative activity in HCT-116 colon cancer cell line. On the basis of docking studies with EGFR hit **1s**, introduction of acrylamide Michael acceptor group led to **8**, which inhibited both the wild and mutant EGFR kinase and also showed antiproliferative activity in HCC827 lung cancer cell line. Furthermore, the X-ray cocrystal study of **3** and **8** in complex with Aurora and EGFR, respectively, confirmed their hypothesized binding modes. Library construction, in situ screening, and structure-based drug design (SBDD) strategy described here could be applied for the lead identification of other kinases.

Introduction

Drug discovery is a complex, risky, costly, and time-consuming process, with estimates for the discovery and development of a drug exceeding 10 years and approximately U.S. $1 billion.[1] Researchers continually seeks methods and technologies to discover drugs more quickly and efficiently. In this context, application of focused library synthesis to speed up both lead identification and optimization is of proven value. However, several caveats for the approaches described so far exist, such as the difficulty of both standardization procedures for solid-phase synthesis and the purification step for solution-phase synthesis. Alternatively solution-phase synthesis followed by in situ screening without the need for isolation of the product has successfully identified potent enzyme inhibitors.[2] These recent methods rely on the identification and application of reactions suitable for carrying out in water-miscible solvent, as after completion of the reaction, the reaction mixture is diluted in water and screened for activity. We here describe our strategies to speed up kinase drug lead identification applied to the design, synthesis, and screening of new compounds, targeting the inhibition of Aurora and epidermal growth factor receptor (EGFR[a]) kinase as an example. Considering the modular nature of the synthesis and screening method, similar protocols could be applied to other protein kinase drug discovery programs.

Protein kinases are enzymes that catalyze the transfer of phosphate groups from adenosine triphosphate (ATP) to sereine, threonine, or tyrosine residues of predetermined target proteins. Phosphorylation of proteins is an important step in cellular signal transduction, regulating cell differentiation, cell growth, and cell migration and influencing apoptotic mechanisms. Deregulation of protein kinase is implicated in a number of diseases, including cancer, diabetes, and inflammation. Thus, targeted inhibition of the deregulated protein kinase has become an attractive therapeutic strategy in cancer therapy.[3] Aurora kinases A, B, and C, members of sereine/threonine kinase, are key mitotic regulators involved in maintaining the genomic integrity of daughter cells. Because overexpression of Aurora A and Aurora B is frequently associated with tumorigenesis, these molecules have been targeted for cancer therapy.[4,5] EGFR, a tyrosine kinase, is overexpressed and also mutated in non-small-cell lung cancer (NSCLC), which leads to aberrant EGFR signaling. Since lung cancer is the leading cause of death due to cancer and 80% of them are NSCLC, targeting EGFR has become a major treatment strategy for NSCLC.[6,7]

Results and Discussion

Through substructure searching for kinase-privileged fragments in our in-house compound library, we found that

†The atomic coordinates and crystal structure have been deposited in the Protein Data Bank as entry 3M11.

*To whom correspondence should be addressed. Phone: +886-37-246-166, extension 35708. Fax: +886-37-586-456. E-mail: hphsieh@nhri.org.tw.

[a]Abbreviations: ATP, adenosine triphosphate; DM, double mutant; EGFR, epidermal growth factor receptor; LCMS, liquid chromatography coupled with mass spectrometry; NSCLC, non-small-cell lung cancer; PDB ID, Protein Data Bank identification number; SBDD, structure-based drug design; WT, wild type.

 Published on Web 06/15/2010

Table 1. Optimization of Screening Protocol for Library Synthesis

Compd	$-NR^1R^2$	Aurora Kinase A % inhibition at 10 μM		Aurora Kinase A IC_{50}[a]
		Library synthesis	Purified sample	
1a	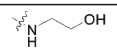	98.2	98.3	0.309
1b	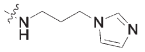	73.8	67.7	3.311
1c		85.8	89.4	0.807
1g	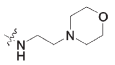	81.7	79.1	1.766
1h	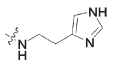	91.4	92.0	0.296

[a] Values are expressed as the mean of at least two independent determinations and are within ±15%.

Scheme 1. Construction of 350 Furanopyrimidine Library Compounds Based on Aurora Hit **1a**[a]

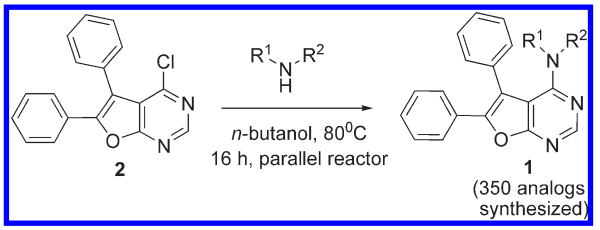

[a] Amines used are shown in Chart 1s of Supporting Information.

compound **1a** (Table 1), which has a furanopyrimidine scaffold, possesses nanomolar (IC_{50} = 309 nM) Aurora kinase A inhibition.[8] To identify compounds with improved potency, we began modification of the hit **1a**. Because preliminary investigation revealed that both the phenyl rings were essential for activity,[8] modification of the side chain was carried out. In general, compound **1** was synthesized by nucleophilic substitution reaction of **2** with various amines in *n*-butanol (Scheme 1). The necessary chloro compound, **2**, was synthesized by a modified procedure reported by Floppe et al.[8,9] Since individual synthesis of the target compound followed by purification would be a time-consuming task, we envisaged synthesizing compounds in a parallel reactor and testing them for Aurora kinase inhibition without purification in a combinatorial fashion. Once compounds with a certain level of activity were identified in this primary screen, they would be resynthesized individually, purified, and retested.

Microtiter-plate-based reaction followed by in situ biochemical estimation of enzyme inhibition without the necessity of isolating the products has been successfully utilized to identify enzyme inhibitors.[2] The key aspect for the successful use of this methodology is the selection of a high-yielding reaction, such as acid amine coupling or 1,3-dipolar addition reaction.[2,10,11] Similarly, we envisaged synthesis and screening protocol, using nucleophilic substitution reaction of amines with 4-chlorofuranopyrimidine **2**. The reaction was carried out in standard glass vials at millimole scale. Two key factors were considered essential for such a work hypothesis: (a) the nucleophilic reaction of various amines with **2** to give the target compound **1** should proceed smoothly and to completion; (b) Aurora kinase A enzyme assay should be specific to the target compounds **1** and should not be influenced by the presence of either the starting material **2** or the amines used.

To test the feasibility of such a library synthesis and in situ screening for activity without purification, we first ran a trial reaction using representative primary amines, secondary amines, aniline derivative, and heterocyclic amines to assess the completion of the nucleophilic reaction. For this purpose, 5 mg of the chloro compound **2**, 4 equiv of the nucleophile, and 1 mL of *n*-butanol were combined in a 5 mL screw-capped vial and heated at 80 °C for 16 h in a parallel reactor. Completion of reaction was assessed by the amount of remaining chloro compound **2** and the formation of desired product using LCMS. It was found that the reactions with both primary amines (**1a**,**b**) and the secondary amine (**1c**) were completed after 16 h of reaction. However, in the case of aniline derivative (**1d**), the reaction was only partially completed and the starting material **2** was observed in LCMS even after prolonged heating for 24 h. In contrast to this, amino acid (**1e**) and heterocyclic amines (**1f**) did not react to give the desired products (Table 1s, Supporting Information). These results showed that only primary and secondary amines were suitable for use as nucleophiles for library synthesis and that for heterocyclic and aniline derivatives alternative synthetic strategies would be essential.

To optimize the screening protocol of the library compounds and to verify potential interference of the excess amine, five compounds (**1a**−**c**,**g**,**h**) were synthesized in the parallel reactor as mentioned above. After 16 h of reaction, *n*-butanol was removed from the reaction mixture under vacuum and the residue obtained was diluted with DMSO to make 10 mM stock samples. The product concentration was considered the same as that of compound **2** because all of the starting material was consumed in the reaction as assessed by LCMS. The five compounds were tested at 10 μM for Aurora A inhibition and showed similar levels of activity as those of the pure compounds, suggesting that assay results were not distorted by the presence of excess amine (Table 1). Moreover

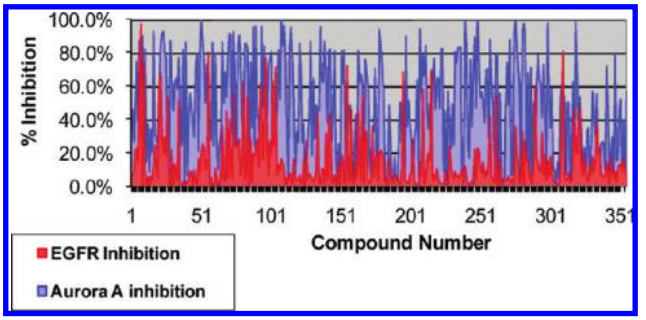

Figure 1. Percentage inhibition of Aurora A (at 10 μM, blue color) and EGFR (at 20 μM, red color) kinase by furanopyrimidine library compounds **1**.

Chart 1. Aurora Kinase A Inhibitors **1i**–**r** and EGFR Kinase Inhibitor **1s** Hits Identified from Library Synthesis with IC_{50} < 1 μM

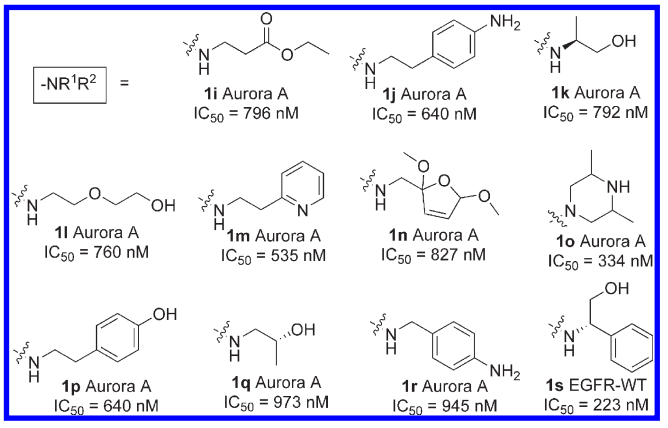

the starting material **2** was found to have 0% inhibition at 10 μM and ~20% inhibition at 50 μM, further supporting the library design and screening protocol.

Having found the right condition for library synthesis and screening protocols, we synthesized around 350 compounds using a variety of primary and secondary amines (Chart 1s, Supporting Information) in the parallel reactor with a maximum capacity of 70 reactions in a single run. To confirm the integrity of the reactions between different runs, compounds **1a** and **1b** were included as internal control in different batches. Screening the compounds as mentioned at 10 μM showed that 46% of the library compounds possessed greater than 50% inhibition at 10 μM and around 20 compounds showed over 90% Aurora inhibition (Figure 1). All 20 compounds were resynthesized, purified, and tested for Aurora inhibition; among them 10 compounds **1i**–**r** (Chart 1) showed submicromolar enzyme inhibition.

Compound **1a** has been cocrystallized in complex with Aurora A and the structure solved by X-ray (Figure 2; PDB ID 3K5U),[8] revealing that the hit binds to the ATP binding pocket with the furanopyrimidine core forming two essential hydrogen bonds with the hinge region. In addition, another hydrogen bond has been observed between the OH group present in the side chain and the Lys172 residue.[8] The two phenyl groups form extensive hydrophobic interaction with the surrounding amino acid residues. Subsequently, the X-ray cocrystal structure of **1i** (data not shown) in complex with Aurora A was also solved, which revealed that the hinge-binding interaction is similar to that of **1a**, while the carbonyl

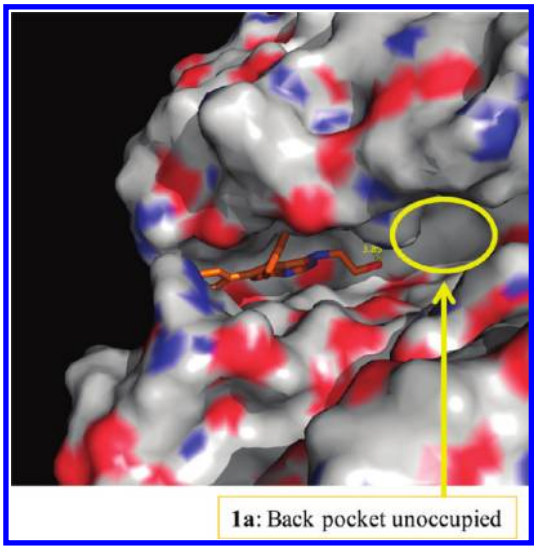

Figure 2. X-ray cocrystal structure of Aurora A protein in complex with inhibitor **1a** (PDB ID 3K5U). Inhibitor **1a** binds to Aurora A using two hydrogen bonds to the hinge region and another hydrogen bond to Lys162. The region commonly referred to as the back pocket (circled yellow) is unoccupied.

Scheme 2. Modification of Library Hit **1j** to Give Analogues **3**–**5**[a]

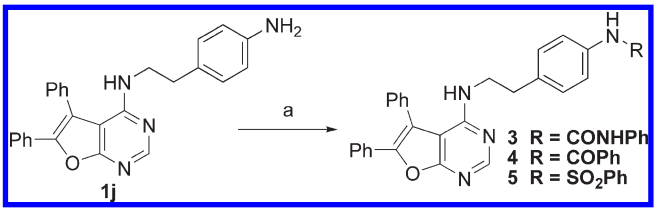

[a] (a) Phenyl isocyanate, CH_2Cl_2, room temp, 8 h for **3**; triethylamine, benzoyl chloride, CH_2Cl_2, room temp, 8 h for **4**; triethylamine, sulfonyl chloride, CH_2Cl_2, room temp, 8 h for **5**.

group of the ester function interacts with the Lys162. Structures **1a** and **1i** both occupy the ATP binding site, commonly referred to in kinase literature as the front cleft/pocket,[12] while the portion commonly referred to as the back cleft/pocket[12] is unoccupied, similar to the situation with ATP binding. The back pocket, which is also referred to as an allosteric site[13] or a deep pocket,[14] has been shown to be occupied by several kinase inhibitors, and exploiting this interaction has been used to enhance the potency and selectivity of the inhibitors to specific kinases.[12–14] On the basis of the similarity in the binding of **1a** and **1i** in Aurora A, we assumed that other potent compounds identified from library synthesis could have a similar binding mode in Aurora A and that all of them have an unoccupied back pocket. Moreover, the side chains of **1a** and **1i** are directed toward the entrance of the back pocket.

On the basis of this structural biology information and the fact that the hits **1i**,**j** possess diverse side chains amenable for further structural modification, we contemplated introduction of functional groups, such as amide, urea, and sulfonamide, common functional groups found among kinase inhibitors that could exploit back-pocket binding.[13,14] With this aim, the aniline functional group of **1j** was converted into urea, amide, and sulfonamide functionality by acylation with phenyl isocyanate, benzoyl chloride, or sulfonyl chloride to give compounds **3**–**5** (Scheme 2). Similarly, the ester function

Scheme 3. Modification of Library Hit **1i** to Give Analogue **6**[a]

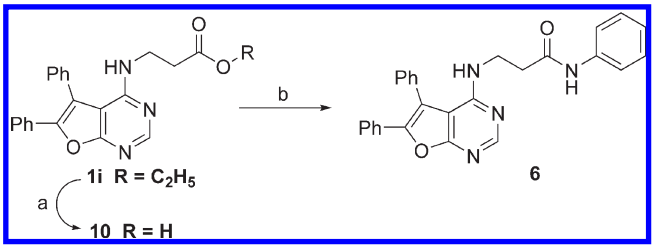

[a] (a) LiOH, MeOH/H_2O (4:1), reflux, 2 h; (b) HOBt, EDC, DMF, aniline, room temp, 16 h.

Table 2. Identification of Potent Aurora Kinase A Inhibitor **3** with Antiproliferative Activity in HCT-116

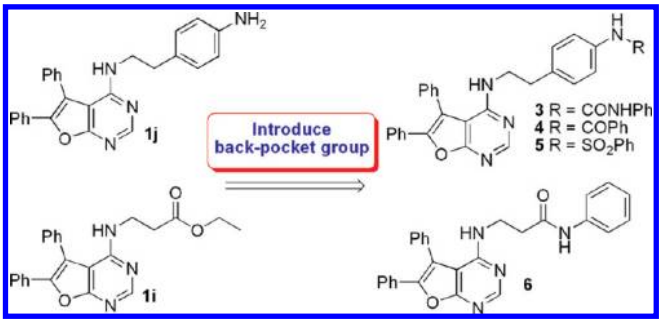

	Aurora based inhibition,[a] IC_{50} (nM)	
compd	Aurora kinase A	HCT-116
1i	796	> 10,000
1j	640	> 10,000
3	43	400
4	304	> 10000
5	5831	> 10000
6	> 10000	> 10000
tozasertib[15]	20	120

[a] Values are expressed as the mean of at least two independent determinations and are within ±15%. Tozasertib (VX-680):[15] Aurora kinase inhibitor tested in phase II clinical trials.

of **1i** was hydrolyzed to the carboxylic acid **10**, which was coupled with aniline to give the amide **6** (Scheme 3).

Compound **3** with the urea functional group showed potent Aurora kinase A inhibition with $IC_{50} \approx 50$ nM. Most importantly, **3** inhibited the growth of the HCT-116 colon cancer cell line in vitro with $IC_{50} \approx 400$ nM (Table 2). Moreover, HCT-116 cells treated with **3** showed the hallmarks of Aurora kinase B inhibition, as evidenced by the DNA content analysis using flow cytometry, which showed a higher percentage of cells with 4N and 8N DNA content (polyploidy) due to failure in cytokinesis. Western blot analysis showed lower levels of posphorylated Aurora A (at Thr288) and histone (H3 at Ser10) proteins, which are Aurora A and B downstream substrates, respectively (Figures 1s and 2s, Supporting Information). These results clearly show that **3** inhibits both Aurora A and B inside the cell. However, the other analogues, **4**−**6**, showed poor Aurora A inhibition and did not inhibit HCT-116 cell growth.

Next, the X-ray cocrystal structure of **3**−Aurora A complex was solved in order to verify if **3** indeed binds to Aurora kinase A as hypothesized. The complex structure shows that **3** binds to Aurora A in a similar way as the initial hit **1a** except that the back pocket of Aurora A is occupied by the terminal phenylurea moiety of **3** (Figure 3; PDB ID 3M11), as hypothesized.

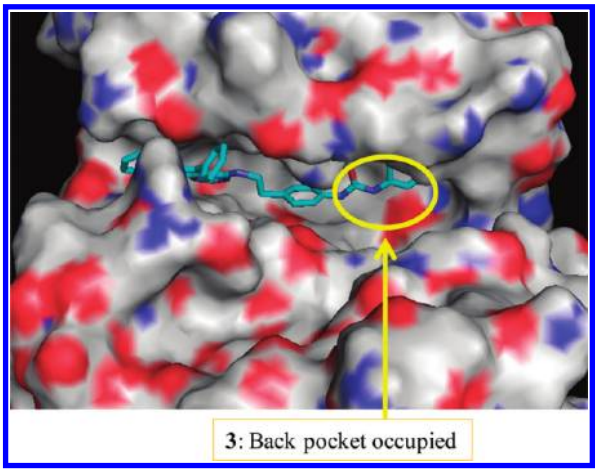

Figure 3. X-ray cocrystal structure of Aurora A protein in complex with inhibitor **3** (PDB ID 3M11). Inhibitor **3** binds to Aurora A using two hydrogen bonds to the hinge region and another hydrogen bond to Lys162. The region commonly referred to as back pocket (circled yellow) is occupied by the terminal phenylurea group.

The urea carbonyl group forms a hydrogen bond with Lys162 of Aurora A, and the terminal phenyl ring of **3** forms hydrophobic contacts with the surrounding residues in the back pocket of Aurora A.

Concurrent with the above Aurora inhibitor development, the library was screened for EGFR kinase inhibition at 20 μM. Most of the compounds were poor inhibitors of EGFR kinase, particularly those that are potent Aurora kinase inhibitors (Figure 1). Three structurally related compounds showed >80% inhibition at 20 μM. Resynthesis identified compound **1s** (Chart 1) as a potent EGFR kinase inhibitor with $IC_{50} \approx 200$ nM, without Aurora kinase inhibition. Structurally **1s** is an *S*-isomer and, when compared to the Aurora hit **1a**, has an additional phenyl group in the side chain. The novel EGFR hit **1s** was evaluated for its ability to inhibit the double mutant (DM, L858R/T790M) EGFR kinase activity, which is resistant to gefitinib (clinically approved treatment for NSCLC), and found to be inactive ($IC_{50} > 10$ μM; Table 3). Identification of compounds that can overcome gefitinib resistant mutant EGFR kinase is therapeutically relevant, as a large number of patients who are initially responsive to gefitinib become resistant over the course of treatment due to emergence of T790M gatekeeper mutation.[7] To aid in this process, we docked **1s** into the active site of the EGFR protein (Figure 4; PDB ID 1M17) cocrystal complex with erlotinib (another clinically approved treatment for NSCLC). The docking results suggest that the furanopyrimidine ring oxygen forms the required hinge binding interaction with the Met769 hinge residue, while the hydroxyl group is within hydrogen bonding distance to Lys721 residue. The three phenyl rings form extensive hydrophobic interaction with the surrounding residues. In addition to this information, modeling results suggest that the phenyl group at the 3-position of the furan ring is suitably positioned to anchor a Michael acceptor group, which could be helpful in improving the activity through covalent modification of the Cys773 residue. It is known that interaction between a suitably positioned Michael acceptor group and the Cys773 residue of the EGFR could improve the EGFR inhibition and also impart activity toward Gefitinib resistant T790M mutant kinase through irreversible covalent bond formation.[7,16,17]

Table 3. Identification of Potent Double Mutant EGFR Kinase Inhibitor **8**

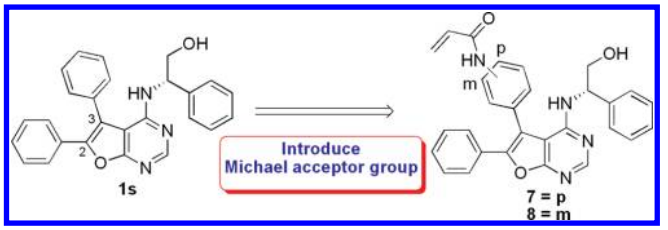

	EGFR based inhibition,[a] IC_{50} nM		
	EGFR kinase		
compd	WT	DM	HCC827
1s	223	> 10000	518
7	82	> 10000	394
8	7[b]	28[b]	8[b]
gefitinib[18]	20[b]	2815	12[b]
9 (BIBW-2992)[19]	11[b]	15[b]	8[b]

[a] Values are expressed as the mean of at least two independent determinations and are within ±15%. [b] Values are expressed as the mean of at least two independent determinations and are within ±25%. WT: wild type EGFR kinase. DM: double mutant (L858R/T790M) EGFR kinase. Gefitinib: reversible EGFR inhibitor used in clinics for the treatment of non-small-cell lung cancer (NSCLC). Compound **9**: irreversible EGFR inhibitor in phase III clinical testing for NSCLC.

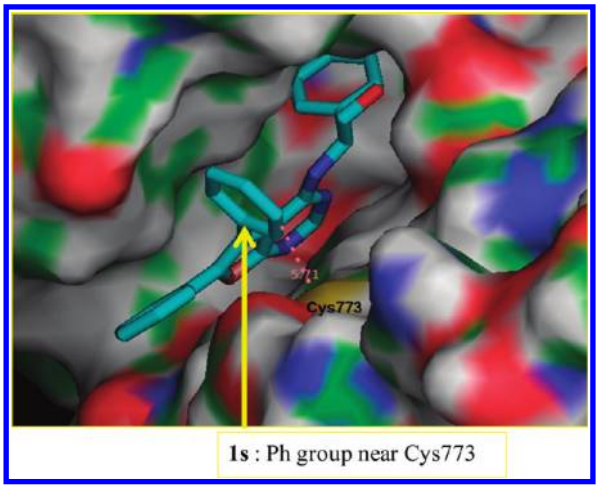

Figure 4. Docking studies of **1s** in active site of EGFR kinase (PDB ID 1M17) cocrystal complex with erlotinib. The 3-phenyl group on the furan ring is close to the Cys773 residue.

On the basis of insights from molecular modeling of **1s**, we introduced an acrylamide Michael acceptor group into the phenyl ring (on the 3-position of the furan ring) of hit **1s** to give compounds **7** and **8** (Scheme 4). It was found that introduction of acrylamide group at the para position of **1s** improved the WT EGFR kinase inhibition around 3-fold for **7**; however, it was inactive toward DM EGFR kinase (IC_{50} > 10 μM; Table 3). Moving the Michael acceptor group from the para to the meta position improved the WT EGFR kinase activity dramatically: over 30-fold for **8**, compared to **1s**. Moreover, the presence of the Michael acceptor group rendered **8** active toward the DM EGFR kinase with an IC_{50} of 28 nM, similar to **9**, which is a second-generation EGFR kinase inhibitor under development for gefitinib-resistant NSCLC. Compound **8** also inhibited the cell growth of HCC827, an NSCLC cell line in the range of single-digit nanomoles. These results suggest that **8** is a novel lead compound with potent

Scheme 4. Synthesis of Furanopyrimidine Analogues **7** and **8**[a]

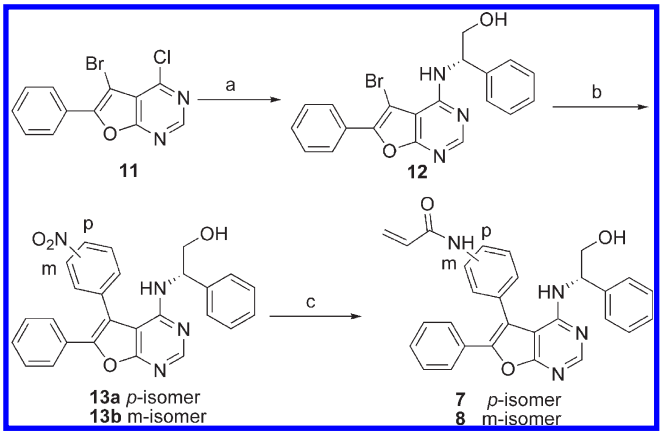

[a] (a) (*S*)-(+)-Phenylglycinol, *n*-butanol, 80 °C, 16 h; (b) $ArB(OH)_2$, $Pd(dppf)_2Cl_2$, Na_2CO_3, dioxane/H_2O, 95 °C, 16 h; (c) H_2, Pd/C, EtOH, atm, 16 h; (i) acryloyl chloride, pyridine, Et_2O, room temp, 16 h.

EGFR kinase inhibition with development potential for gefitinib-resistant EGFR overexpressing tumors.

We further confirmed that the designed-in Michael acceptor group of **8** could covalently interact with the Cys773 residue by solving the X-ray cocrystal complex of **8** with EGFR kinase (Figure 3s, Supporting Information). A clear covalent linkage between the Michael acceptor group of **8** and Cys773 residue sulfur atom of EGFR protein was observed, which would result in irreversible inhibition of EGFR kinase, explaining the potent activity of **8**, compared to the hit **1s**. Furthermore, the molecule was also anchored by a hydrogen bond interaction between the furan ring oxygen and Met769 of hinge region. (However, it is noted that some parts of the ligand (phenyl group) were not clear in the density map, indicating that they might be flexible in the EGFR pocket, precluding deposition of the coordinates to PDB.)

Conclusion

In summary, through rapid construction of a furanopyrimidine kinase-targeted library and screening it without isolation of the compounds, several synthetically tractable and structurally distinct leads for Aurora and EGFR kinase inhibition were quickly identified. Potent hits identified from the library were further modified based on structure biology/docking studies in the kinase. On the basis of the structural insight that the region commonly referred to as back pocket in Aurora kinase A is unoccupied by Aurora hit **1a**, functional groups that could interact in the back pocket were introduced. This drug-design strategy led to the identification of potent Aurora kinase A inhibitor **3**, which has antiproliferative activity in the HCT-116 colon cancer cell line. Docking study of the EGFR hit **1s** from the library revealed possible enhancement of EGFR kinase activity through the introduction of Michael acceptor functionality. On the basis of this finding, introduction of acrylamide Michael acceptor group led to the synthesis of **8**, which showed potent activity in both wild and mutant EGFR kinase, with potent antiproliferative activity in HCC827 lung cancer cell line. X-ray cocrystal complex of **3** with Aurora kinase A showed that the back pocket is occupied by the inhibitor **3**, while X-ray cocrystal complex of **8** with EGFR kinase showed the presence of a covalent bond between the Michael acceptor region of the inhibitor and Csy733 residue of EGFR, as predicted. Thus, library construction, in situ screening, and structure-based drug design provided a

tool to identify compounds with the same scaffold but displaying distinct biological target/activities. Both **3** and **8** are potential leads that are development candidates in our drug discovery program. In addition, the library compounds could be subjected to screening to identify suitable hits to act as starting points for a lead-optimization program for other therapeutically relevant kinases. Moreover, such a library-construction and screening approach could be applied to different core structures known to possess kinase hinge region binding, thereby allowing effective exploration of kinome chemical space.

Experimental Section

General Methods. All commercial chemicals and solvents are reagent grade and were used without further treatment unless otherwise noted. All reactions were carried out under an atmosphere of dry nitrogen. Reactions were monitored by TLC using Merck 60 F_{254} silica gel glass backed plates (5 cm × 10 cm); zones were detected visually under ultraviolet irradiation (254 nm) or by spraying with phosphomolybdic acid reagent (Aldrich) followed by heating at 80 °C. Flash column chromatography was done using silica gel (Merck Kieselgel 60, no. 9385, 230−400 mesh ASTM). ^{1}H and ^{13}C NMR spectra were obtained with a Varian Mercury-300 or Varian Mercury-400 spectrometer. Chemical shifts were recorded in parts per million (ppm, δ) and were reported relative to the solvent peak or TMS. High-resolution mass spectra (HRMS) were measured with a Finnigan (MAT-95XL) electron impact (EI) mass spectrometer or using Finnigan/Thermo Quest MAT 95XL FAB mass spectrometer. LCMS data were measured on an Agilent MSD-1100 ESI-MS/MS system. Parallel synthesis was carried out in parallel block reactors (KEM Scientific Inc.), and the solvents were evaporated in a Savant SpeedVac Plus system. The purity of the final compounds was determined using a Hitachi 2000 series HPLC system using a C-18 column (Agilent ZORBAX Eclipse XDB-C18 5 μm, 4.6 mm × 150 mm) and was found to be >95% unless otherwise stated.

Parallel Synthesis Protocol. The chloro compound **2** (5 mg) was taken into a 5 mL screw-capped vial, and 4 equiv of the nucleophile/amine and *n*-butanol (1 mL) were added. The mixture was heated at 80 °C for 16 h in a parallel block reactor. After reaction completion, *n*-butanol was removed from the reaction mixture under vacuum, and the residue obtained was diluted with DMSO to make 10 mM stock samples and tested at 10 μM for Aurora A inhibition and at 20 μM for EGFR inhibition.

Synthesis of Pure Furanopyrimidine Analogues 1b,c,g−s. Pure compounds **1b**,**c**,**g**−**s** were prepared from 4-chloro-5,6-diphenylfuro[2,3-*d*]pyrimidine (**2**) and appropriate amines in 70−90% yield in a manner similar to that of **1a** reported by us.[8]

(5,6-Diphenylfuro[2,3-*d*]pyrimidin-4-yl)-(3-imidazol-1-ylpropyl)-amine 1b. ^{1}H NMR (300 MHz, $CDCl_3 + CD_3OD$): δ 8.31 (s, 1H), 7.68 (s, 1H), 7.54−7.51 (m, 3 H), 7.46−7.43 (m, 4H), 7.24−7.20 (m, 3H), 7.03 (s, 1H), 6.90 (s, 1H), 3.95−3.90 (t, J = 6.6 Hz, 2H), 3.39−3.32 (m, 2H), 1.97−1.92 (m, 2H). HRMS (EI): calcd for $C_{24}H_{21}N_5O$ 395.1746, found 395.1746.

1-(5,6-Diphenylfuro[2,3-*d*]pyrimidin-4-yl)piperidin-4-ol 1c. ^{1}H NMR (300 MHz, $CDCl_3$): δ 8.52 (s, 1H), 7.51−7.41 (m, 8H), 7.40−7.27 (m, 2H), 3.76−3.71 (m, 1H), 3.67−3.59 (m, 2H), 3.03−2.97 (m, 2H), 1.63−1.59 (m, 2H), 1.30−1.18 (m, 2H). HRMS (EI): calcd for $C_{23}H_{21}N_3O_2$ 371.1634, found 371.1628.

(5,6-Diphenylfuro[2,3-*d*]pyrimidin-4-yl)-(2-morpholin-4-ylethyl)-amine 1g. ^{1}H NMR (300 MHz, $CDCl_3$): δ 8.42 (s, 1H), 7.58−7.47 (m, 7 H), 7.28−7.24 (m, 3H), 5.36 (s, 1H), 3.57−3.56 (m, 6H), 2.50−2.34 (m, 6H). ^{13}C NMR (75 MHz, $CDCl_3$): δ 165.1 (C), 157.6 (C), 154.3 (C), 147.0 (C), 132.6 (C), 130.1 (CH), 129.8 (CH), 129.7 (C), 129.1 (CH), 128.7 (CH), 128.6 (CH), 126.6 (CH), 115.2 (C), 77.4 (CH), 66.5 (CH_2), 56.7 (CH_2), 53.2 (CH_2), 37.1 (CH_2). LCMS (ESI) m/z 401.5 $(M + H)^+$.

(5,6-Diphenylfuro[2,3-*d*]pyrimidin-4-yl)-[2-(1*H*-imidazol-4-yl)-ethyl]amine 1h. ^{1}H NMR (300 MHz, $CDCl_3 + CD_3OD$): δ 8.30 (s, 1H), 7.81 (s, 1H), 7.46−7.39 (m, 5 H), 7.36−7.33 (m, 2H), 7.21−7.19 (m, 3H), 6.61 (s, 1H), 3.65−3.60 (t, J = 6.6 Hz, 2H), 2.77−2.73 (t, J = 6.6 Hz, 2H). LCMS (ESI) m/z 382.4 $(M + H)^+$.

3-(5,6-Diphenylfuro[2,3-*d*]pyrimidin-4-ylamino)propionic Acid Ethyl Ester 1i. ^{1}H NMR (300 MHz, $CDCl_3$): δ 8.41 (s, 1H), 7.56−7.44 (m, 8H), 7.28−7.24 (m, 2H), 5.16−5.13 (t, J = 5.4 Hz, 1H), 4.11−4.04 (q, J = 7.2 Hz, 2H), 3.76−3.70 (q, J = 6.0 Hz, 2H), 2.57−2.53 (t, J = 6.0 Hz, 2H), 1.23−1.18 (t, J = 7.2 Hz, 3H). HRMS (EI): calcd for $C_{23}H_{21}N_3O_3$ 387.1583, found 387.1580.

[2-(4-Aminophenyl)ethyl]-(5,6-diphenylfuro[2,3-*d*]pyrimidin-4-yl)-amine 1j. ^{1}H NMR (300 MHz, $CDCl_3$): δ 8.43 (s, 1H), 7.50−7.23 (m, 10H), 6.79 (d, J = 8.4 Hz, 2H), 6.59 (d, J = 8.4 Hz, 2H), 4.68 (t, J = 5.2 Hz, 1H), 3.65 (q, J = 6.4 Hz, 2H), 3.62 (bs, 2H), 2.67 (t, J = 6.4 Hz, 2H). ^{13}C NMR (100 MHz, $CDCl_3$): δ 164.9 (C), 157.5 (C), 154.2 (CH), 146.5 (C), 144.8 (C), 132.3 (C), 129.6 (CH), 129.5 (CH), 129.4 (CH), 128.7 (CH), 128.4 (CH), 128.3 (CH), 126.3 (CH), 115.4 (CH), 115.0 (C), 103.1 (C), 42.1 (CH_2), 34.2 (CH_2). HRMS (EI) calcd. for $C_{26}H_{22}N_4O$ 406.1794, found 406.1789.

***S*-2-(5,6-Diphenylfuro[2,3-*d*]pyrimidin-4-ylamino)propan-1-ol 1k.** ^{1}H NMR (300 MHz, $CDCl_3$): δ 8.40 (s, 1H), 7.61−7.49 (m, 8 H), 7.32−7.27 (m, 2H), 4.86 (bs, 1H), 3.72−3.68 (m, 1H), 3.44−3.38 (m, 1H), 1.11 (d, J = 6.3 Hz, 3H). HRMS (EI) calcd for $C_{21}H_{19}N_3O_2$ 345.1477, found 345.1474.

2-[2-(5,6-Diphenylfuro[2,3-*d*]pyrimidin-4-ylamino)ethoxy]ethanol 1l. ^{1}H NMR (300 MHz, $CDCl_3$): δ 8.41 (s, 1H), 7.59−7.50 (m, 8H), 7.27−7.24 (m, 2H), 5.06 (bs, 1H), 3.69−3.59 (m, 4H), 3.54 (t, J = 5.1 Hz, 2H), 3.44 (t, J = 4.5 Hz, 2H), 1.77 (bt, J = 6.0 Hz, 1H). HRMS (EI) calcd for $C_{22}H_{21}N_3O_3$ 375.1583, found 375.1575.

(5,6-Diphenylfuro[2,3-*d*]pyrimidin-4-yl)-(2-pyridin-2-ylethyl)-amine 1m. ^{1}H NMR (300 MHz, $CDCl_3$): δ 8.42 (s, 1H), 8.32 (d, J = 3.9 Hz, 1H), 7.57−7.52 (m, 1H), 7.48−7.32 (m, 8H), 7.25−7.22 (m, 2H), 7.12−7.08 (m, 1H), 7.02 (d, J = 7.5 Hz, 1H), 5.29 (bt, J = 6.6 Hz, 1H), 3.90 (q, J = 6.0 Hz, 2H), 2.98 (t, J = 6.3 Hz, 2H). LCMS (ESI) m/z 393.1 $(M + H)^+$. HPLC purity, 94.7%.

(2,5-Dimethoxy-2,5-dihydrofuran-2-ylmethyl)-(5,6-diphenylfuro-[2,3-*d*]pyrimidin-4-yl)amine 1n. ^{1}H NMR (400 MHz, $CDCl_3$): δ 8.40 (s, 1H), 7.56−7.48 (m, 7H), 7.28−7.23 (m, 3H), 7.00 (dd, J = 6.0, 1.2 Hz, 1H), 5.81 (dd, J = 6.0, 0.8 Hz, 1H), 5.67 (dd, J = 1.2, 0.8 Hz, 1H), 5.07 (bt, J = 5.6 Hz, 1H), 3.85 (dd, J = 13.6, 6.4 Hz, 1H), 3.78 (dd, J = 13.6, 5.2 Hz, 1H), 3.22 (s, 3H), 3.04 (s, 3H). HRMS (EI) calcd for $C_{25}H_{23}N_3O_4$ 429.1689, found 429.1686. HPLC purity, 94.9%.

4-(3,5-Dimethylpiperazin-1-yl)-5,6-diphenylfuro[2,3-*d*]pyrimidine 1o. ^{1}H NMR (400 MHz, $CDCl_3$): δ 8.48 (s, 1H), 7.49−7.40 (m, 8H), 7.28−7.24 (m, 2H), 3.73−3.69 (m, 2H), 2.54−2.47 (m, 2H), 2.22 (dd, J = 12.4, 10.8 Hz, 2H), 0.81 (d, J = 6.4 Hz, 6H). ^{13}C NMR (100 MHz, $CDCl_3$): δ 166.9 (C), 160.6 (C), 152.5 (CH), 147.6 (C), 133.5 (C), 130.3 (CH), 129.6 (C), 129.2 (CH), 128.5 (CH), 128.3 (CH), 128.2 (CH), 127.1 (CH), 115.7 (C), 105.6 (C), 55.5 (CH_2), 50.1 (CH), 19.2 (CH_3). HRMS (EI) calcd for $C_{24}H_{24}N_4O$ 384.1950, found 384.1943.

4-[2-(5,6-Diphenylfuro[2,3-*d*]pyrimidin-4-ylamino)ethyl]phenol 1p. ^{1}H NMR (300 MHz, $CDCl_3$): δ 8.43 (s, 1H), 7.49−7.36 (m, 6H), 7.32−7.23 (m, 4H), 6.89 (d, J = 9.0 Hz, 2H), 6.74 (d, J = 9.0 Hz, 2H), 4.65 (bt, J = 5.1 Hz, 1H), 3.68 (q, J = 6.0 Hz, 2H), 2.71 (t, J = 6.3 Hz, 2H). HRMS (EI) calcd for $C_{26}H_{21}N_3O_2$ 407.1634, found 407.1629.

1-(5,6-Diphenylfuro[2,3-*d*]pyrimidin-4-ylamino)propan-2-ol 1q. ^{1}H NMR (300 MHz, $CDCl_3$): δ 8.34 (s, 1H), 7.54−7.46 (m, 8 H), 7.25−7.22 (m, 2H), 5.06 (bt, J = 5.1 Hz, 1H), 3.92−3.86 (m, 1H), 3.58−3.51 (m, 1H), 3.32−3.23 (m, 1H), 1.11 (d, J = 6.6 Hz, 3H). LCMS (ESI) m/z 346.1 $(M + H)^+$.

(4-Aminobenzyl)-(5,6-diphenylfuro[2,3-*d*]pyrimidin-4-yl)amine 1r. ^{1}H NMR (300 MHz, $CDCl_3$): δ 8.44 (s, 1H), 7.53−7.44 (m, 8H), 7.26−7.25 (m, 2H), 6.93 (d, J = 7.2 Hz, 2H), 6.61 (d, J = 7.2 Hz, 2H), 4.88 (bs, 1H), 4.51 (d, J = 3.6 Hz, 2H), 3.26 (bs, 2H). HRMS (EI) calcd for $C_{25}H_{20}N_4O$ 392.1637, found 392.1634.

***S*-2-(5,6-Diphenylfuro[2,3-*d*]pyrimidin-4-ylamino)-2-phenylethanol 1s.** ^{1}H NMR (300 MHz, $CDCl_3$): δ 8.40 (s, 1H), 7.59−7.28 (m, 13 H), 7.04−7.00 (m, 2H), 5.36 (bd, J = 6.0 Hz, 1H), 5.30−5.24 (m, 1H), 3.86−3.74 (m, 2H). LCMS (ESI) m/z 408.2 $(M + H)^+$.

1-{4-[2-(5,6-Diphenylfuro[2,3-*d*]pyrimidin-4-ylamino)ethyl]phenyl}-3-phenylurea 3. To a solution of compound **1j** (50 mg, 0.123 mmol) in CH_2Cl_2 (5 mL) was added phenyl isocyanate (18 mg, 0.147 mmol). The mixture was stirred for 8 h at room temperature. Then water (10 mL) was added and extracted with CH_2Cl_2 (3 × 10 mL). The combined organic layers were dried over $MgSO_4$ and concentrated under reduced pressure. The residue was purified by gradient flash column chromatography on silica gel (acetone/CH_2Cl_2 = 1:25 to MeOH/CH_2Cl_2 = 1:50) to furnish **3** (59 mg, 92%). ^{1}H NMR ($CDCl_3$, 300 MHz): δ 8.43 (s, 1H), 7.48−7.22 (m, 16H), 7.12 (tt, J = 6.8, 2.0 Hz, 1H), 6.95 (d, J = 8.4 Hz, 2H), 6.72 (bs, 2H), 4.66 (bt, J = 5.2 Hz, 1H), 3.69 (q, J = 6.4 Hz, 2H), 2.75 (t, J = 6.4 Hz, 2H). ^{13}C NMR (100 MHz, $CDCl_3$): δ 164.5 (C), 157.4 (C), 154.0 (C), 153.8 (CH), 146.6 (C), 138.4 (C), 136.9 (C), 133.3 (C), 131.8 (C), 129.6 (CH), 129.4 (CH), 129.1 (C), 129.0 (CH), 128.9 (CH), 128.4 (CH), 126.2 (CH), 123.3 (CH), 120.4 (CH), 120.2 (CH), 114.1 (C), 103.1 (C), 41.9 (CH_2), 34.3 (CH_2). HRMS (FAB) calcd for $C_{33}H_{27}N_5O_2$ 525.2165, found 526.2249 $(M + H)^+$.

***N*-{4-[2-(5,6-Diphenylfuro[2,3-*d*]pyrimidin-4-ylamino)ethyl]phenyl}benzamide 4.** To a solution of compound **1j** (50 mg, 0.123 mmol) and triethylamine (25 mg, 0.246 mmol) in CH_2Cl_2 (5 mL) was added benzoyl chloride (26 mg, 0.184 mmol), and the mixture was stirred for 8 h at room temperature. Then water (10 mL) was added and extracted with CH_2Cl_2 (3 × 10 mL). The combined organic layers were dried over $MgSO_4$ and concentrated under reduced pressure. The residue was purified by gradient flash column chromatography on silica gel (EtOAc/hexane = 1:10 to MeOH/CH_2Cl_2 = 1:50) to furnish **4** (53 mg, 85%). ^{1}H NMR (400 MHz, $CDCl_3$): δ 8.44 (s, 1H), 7.90 (d, J = 8.0 Hz, 2H), 7.79 (bs, 1H), 7.23−7.60 (m, 15H), 7.02 (d, J = 8.0 Hz, 2H), 4.67 (bt, J = 5.2 Hz, 1H), 3.72 (q, J = 6.4 Hz, 2H), 2.80 (t, J = 6.4 Hz, 2H). ^{13}C NMR (100 MHz, $CDCl_3$): δ 165.8 (C), 164.7 (C), 157.3 (C), 154.0 (CH), 146.5 (C), 136.4 (C), 134.8 (C), 134.7 (C), 132.0 (C), 131.8 (CH), 129.6 (CH), 129.5 (CH), 129.3 (C), 129.1 (CH), 128.8 (CH), 128.7 (CH), 128.4 (CH), 128.3 (CH), 127.0 (CH), 126.2 (CH), 120.5 (CH), 114.8 (C), 103.1 (C), 41.8 (CH_2), 34.4 (CH_2). HRMS (EI) calcd. for $C_{33}H_{26}N_4O_2$ 510.2056, found 510.2055.

***N*-{4-[2-(5,6-Diphenylfuro[2,3-*d*]pyrimidin-4-ylamino)ethyl]phenyl}benzenesulfonamide 5.** To a solution of compound **1j** (50 mg, 0.123 mmol) and triethylamine (25 mg, 0.246 mmol) in CH_2Cl_2 (5 mL) was added benzenesulfonyl chloride (32 mg, 0.184 mmol) and the mixture stirred for 8 h at room temperature. Then water (10 mL) was added and extracted with CH_2Cl_2 (3 × 10 mL). The combined organic layers were dried over $MgSO_4$ and concentrated under reduced pressure. The residue was purified by gradient flash column chromatography on silica gel (acetone/CH_2Cl_2 = 1:25 to MeOH/CH_2Cl_2 = 1:10) to furnish **5** (60 mg, 90%). ^{1}H NMR (400 MHz, $CDCl_3$): δ 8.42 (s, 1H), 7.77 (d, J = 8.4 Hz, 2H), 7.46−7.53 (m, 3H), 7.34−7.43 (m, 5H), 7.24−7.27 (m, 5H), 6.96 (d, J = 8.4 Hz, 2H), 6.88 (d, J = 8.4 Hz, 2H), 6.70 (bs, 1H), 4.59 (bt, J = 5.2 Hz, 1H), 3.66 (q, J = 6.4 Hz, 2H), 2.71 (t, J = 6.4 Hz, 2H). ^{13}C NMR (100 MHz, $CDCl_3$): δ 164.6 (C),157.3 (C), 154.0 (CH), 146.5 (C), 139.2 (C), 135.5 (C), 135.0 (C), 132.9 (C), 132.0 (C), 129.6 (CH), 129.4 (CH), 129.3 (CH), 129.3 (C), 129.0 (CH), 128.8 (CH), 128.4 (CH), 127.1 (CH), 126.2 (CH), 121.7 (CH), 114.8 (CH), 103.1 (C), 41.6 (CH_2), 34.3 (CH_2). HRMS (EI) calcd for $C_{32}H_{26}N_4O_3S$ 546.1726, found 546.1729.

3-(5,6-Diphenylfuro[2,3-*d*]pyrimidin-4-ylamino)propionic Acid 10. LiOH (18 mg, 0.78 mmol) was added to a solution of **1i** (100 mg, 0.26 mmol) in a mixture of 10 mL of methanol/water (4:1) and refluxed for 2 h. Solvents were removed under vacuum. Water was added, and the mixture was neutralized with dilute HCl and extracted with ethyl acetate (3 × 20 mL). The organic layers were combined, washed with water and then brine, and dried over $MgSO_4$. Removal of solvents under vacuum provided crude product **10** (83 mg, 90%). ^{1}H NMR (300 MHz, $CDCl_3$ + CD_3OD): δ 8.43 (s, 1H), 7.55−7.41 (m, 8H), 7.28−7.24 (m, 2H), 3.77 (t, J = 6.0 Hz, 2H), 2.6 (t, J = 6.0 Hz, 2H). LCMS (ESI) m/z 360.1 $(M + H)^+$.

3-(5,6-Diphenylfuro[2,3-*d*]pyrimidin-4-ylamino)-*N*-phenylpropionamide 6. *N*-Hydroxybenzotriazole (34 mg, 0.22 mmol) and 1-(3-dimethylaminopropyl)-3-ethylcarbodiimide hydrochloride (42 mg, 0.22 mmol) were added to a solution of **10** (80 mg, 0.22 mmol) in anhydrous DMF (4.0 mL), and the mixture was stirred under nitrogen atmosphere for 1 h at room temperature. Then aniline (30 mg, 0.32 mmol) was added, with continued stirring for 16 h. After completion of the reaction, water was added and extracted with ethyl acetate (3 × 30 mL). The organic layers were combined, washed with water (2 × 20 mL) and then brine, and dried over $MgSO_4$. Removal of solvents under vacuum provided crude product, which was purified on silica gel flash column chromatography using EtOAc/hexane = 3:7 to give **6** (70 mg, 72%). ^{1}H NMR (300 MHz, $CDCl_3$): δ 8.55 (s, 1H), 8.36 (s, 1H), 7.65−7.62 (m, 2H), 7.42−7.29 (m, 8H), 7.22−7.08 (m, 5H), 5.19 (bs, 1H), 3.80 (q, J = 6.0 Hz, 2H), 2.68 (t, J = 6.0 Hz, 2H). LCMS (ESI) m/z: 435.2 $(M + H)^+$. HPLC purity, 92.6%.

2-(5-Bromo-6-phenylfuro[2,3-*d*]pyrimidin-4-ylamino)-2-phenylethanol 12. Compound **12** was synthesized in 69% yield from **11**[8] and (*S*)-(+)-phenylglycinol using similar reaction conditions as those for compound **1**. ^{1}H NMR (300 MHz, $CDCl_3$): δ 8.30 (s, 1H), 8.07−8.02 (m, 2H), 7.51−7.30 (m, 8H), 6.89 (d, J = 6.9 Hz, 1H), 5.50−5.45 (m, 1H), 4.05 (d, J = 4.8 Hz, 2H), 3.39 (brs, 1H). LCMS (ESI) m/z 411.1 $(M + H)^+$.

2-[5-(4-Nitrophenyl)-6-phenylfuro[2,3-*d*]pyrimidin-4-ylamino]-2-phenylethanol 13a. A mixture of compound **12** (410 mg, 1.0 mmol) and *p*-nitrobenzeneboronic acid (195 mg, 1.2 mmol) was dissolved in dioxane (2.0 mL) under a nitrogen atmosphere. $Pd(dppf)_2Cl_2$ (4.2 mg, 0.05 mmol) and Na_2CO_3 solution (2 M, 1.0 mL) were added to this mixture and heated at 95 °C for 16 h under nitrogen. After completion, the reaction mixture was cooled to room temperature, water was added, and the mixture was extracted with ethyl acetate (3 × 20 mL). Combined organics were dried over $NaSO_4$, concentrated under vacuum, and the residue obtained was purified over silica gel flash column chromatography using hexane/ethyl acetate = 1:1 to give **13a** (346 mg, 77%). ^{1}H NMR (300 MHz, $CDCl_3$): δ 8.41 (s, 1H), 8.29 (d, J = 8.4 Hz, 2H), 7.67 (d, J = 8.4 Hz, 2H), 7.50−7.47 (m, 2H), 7.34−7.26 (m, 6H), 7.09−7.05 (m, 2H), 5.23 (dd, J = 10.2, 5.4 Hz, 1H), 5.16 (d, J = 5.4 Hz, 1H), 3.88−3.84 (m, 2H), 3.31 (*t*, J = 5.4 Hz, 1H). LCMS (ESI) m/z 453.1 $(M + H)^+$.

2-[5-(3-Nitrophenyl)-6-phenylfuro[2,3-*d*]pyrimidin-4-ylamino]-2-phenylethanol 13b. Compound **13b** was synthesized in 75% yield in a manner similar to that for **13a**, using *m*-nitrobenzeneboronic acid. ^{1}H NMR (300 MHz, $CDCl_3$): δ 8.41 (s, 2H), 8.30 (ddd, J = 8.1, 1.2, 1.2 Hz, 1H), 7.82 (dd, J = 7.8, 1.2 Hz, 1H), 7.65 (dd, J = 8.1, 7.8 Hz, 1H), 7.50−7.47 (m, 2H), 7.34−7.26 (m, 6H), 7.11−7.07 (m, 2H), 5.27−5.20 (m, 2H), 3.88−3.84 (m, 2H), 3.31 (*t*, J = 5.4 Hz, 1H). LCMS (ESI) m/z 453.1 $(M + H)^+$.

***N*-{4-[4-(2-Hydroxy-1-phenylethylamino)-6-phenylfuro[2,3-*d*]pyrimidin-5-yl]phenyl}acrylamide 7.** A mixture of **13a** (136 mg, 0.3 mmol) and 5% Pd/C (10 mg) in EtOH (3 mL) was hydrogenated at atmospheric pressure for 16 h. The reaction mixture was filtered over Celite, and the solvents removed under vacuum to give 2-[5-(4-aminophenyl)-6-phenylfuro[2,3-*d*]pyrimidin-4-ylamino]-2-phenylethanol. Acryloyl chloride (0.03 mL, 0.33 mmol) was added to a mixture of the above compound and pyridine (0.05 mL, 0.6 mmol) in a solution of ether (3 mL). The reaction mixture was then stirred at room temperature for 16 h. After completion of the reaction, water was added and extracted with ethyl acetate (3 × 20 mL). The combined organics were

dried over $MgSO_4$, concentrated under vacuum and the residue was purified over silica gel flash column chromatography using hexane/ethyl acetate = 2:3 to give **7** (29 mg, 20%). ^{1}H NMR (300 MHz, $CDCl_3$) δ 8.33 (s, 1H), 8.00 (brs, 1H), 7.80−7.71 (m, 2H), 7.57 (d, J = 8.4 Hz, 2H), 7.47−7.44 (m, 3H), 7.30−7.19 (m, 5H), 7.07 (d, J = 8.4 Hz, 2H), 6.50 (d, J = 16.8 Hz, 1H), 6.32 (dd, J = 16.8, 10.2 Hz, 1H), 5.83 (d, J = 10.2 Hz, 1H), 5.45 (d, J = 6.3 Hz, 1H), 5.20−5.18 (m, 1H), 3.86−3.73 (m, 2H). LCMS (ESI) m/z 477.1 $(M + H)^+$. HPLC purity, 90.4%.

***N*-{3-[4-(2-Hydroxy-1-phenylethylamino)-6-phenylfuro[2,3-*d*]-pyrimidin-5-yl]phenyl}acrylamide 8.** Compound **8** was synthesized in 25% yield from **13b** in a manner similar to that for **7**. ^{1}H NMR (300 MHz, $CDCl_3$): δ 8.58 (brs, 1H), 8.27 (s, 1H), 7.79−7.64 (m, 2H), 7.49−7.46 (m, 2H), 7.40 (t, J = 7.5 Hz, 1H), 7.27−7.20 (m, 8H), 7.05−7.02 (d, J = 7.5 Hz, 2H), 6.46 (d, J = 16.8 Hz, 1H), 6.28 (dd, J = 16.8, 10.2 Hz, 1H), 5.73 (d, J = 10.2 Hz, 1H), 5.64 (d, J = 6.0 Hz, 1H), 5.30 (brs, 1H), 3.86 (dd, J = 11.4, 2.7 Hz, 1H), 3.69 (dd, J = 11.4, 6.9 Hz, 1H). HRMS (EI) calcd for $C_{29}H_{24}N_4O_3$ 476.1848, found 476.1843.

Aurora Kinase A Assay. Aurora kinase A enzyme inhibition assay was performed as reported by us earlier.[20]

EGFR WT/DM Kinase Assay. This assay was performed by modification of the method reported by us earlier.[21] GST-EGFR-KD^{WT} containing the EGFR kinase catalytic domain (residues 696−1022) and GST-EGFR-KD$^{L858R/T790M}$ containing the EGFR kinase catalytic domain (residues from 696 to 1022 and with L858R/T790M) were expressed in Sf9 insect cells transfected with baculovirus containing pBac-PAK8-GST-EGFR-KD plasmid, respectively. GST-EGFR-KD^{WT} protein expression and purification and kinase assay were done in a manner as reported earlier.[21] The EGFR$^{L858R/T790M}$ Kinase-Glo assays were carried out in 96-well plates at 37 °C for 60 min in a final volume of 50 μL, including the following components: 200 ng of GST-EGFR-KD$^{L858R/T790M}$ proteins, 25 mM HEPES, pH 7.4, 4 mM $MnCl_2$, 2 mM DTT, 10 mM $MgCl_2$, 0.1 mg/mL bovine serum albumin, 10 μM poly(Glu,Tyr) 4:1, 0.5 mM Na_3VO_4, and 1 μM ATP. Following incubation, 50 μL Kinase-Glo Plus reagent (Promega) was added, and the mixture was incubated at 25 °C for 20 min. A 70 μL aliquot of each reaction mixture was transferred to a black microtiter plate, and the luminescence was measured using a Wallac Vector 1420 multilabel counter (PerkinElmer).

HCT-116 Antiproliferative Assay. HCT-116 cell viability was examined by MTS assay (Promega, Madison, WI). Two-thousand HCT-116 cells in 100 μL of McCoy's 5a medium were seeded in each well of a 96-well plate. After 96 h of incubation with a test compound, the cells were incubated with 20 μL of a MTS/PMS mixture (MTS/PMS ratio of 20:1) for 2 h at 37 °C in a humidified incubator with 5% CO_2 to allow viable cells to convert the tetrazolium salt (MTS) into formazan. The amount/concentration of formazan, which indicates the number of live cells, was determined by measuring the absorbance at 490 nm using a PerkinElmer Victor2 plate reader (PerkinElmer, Shelton, CT).

HCT-116 Flow Cytometry Analysis. Flow cytometry analysis of HCT-116 cells treated with compound **3** was performed as follows. HCT116 cells were seeded at low confluency in six-well plates and treated with compounds or DMSO for 48 h. Cells were harvested and stained with 0.1% propidium iodide (Sigma Aldrich) hypotonic buffer at 4 °C for 15 min. Samples were subjected to flow cytometry (FACS Calibus, BD) to measure DNA content of the cells (FL2-A). Cell cycle profiling was analyzed by CellQuest Pro.

HCT-116 Western Blot Analysis. Western blot analysis of HCT-116 cells treated with compound **3** was performed as reported by us earlier.[22]

HCC-827 Antiproliferative Assay. HCC827 cell viability was examined by MTS assay (Promega, Madison, WI). One-thousand HCC827 cells in 100 μL of RPMI1640 with 10% FBS medium were seeded in each well of a 96-well plate. After 96 h of incubation with the test compound, the cells were further incubated with 20 μL of a MTS/PMS mixture (MTS/PMS ratio of 20:1) in each well of the 96-well plate for 2 h at 37 °C in a humidified incubator with 5% CO_2 to allow viable cells to convert the tetrazolium salt (MTS) into formazan. The amount/concentration of formazan, which indicates the number of live cells, was determined by measuring its absorbance at 490 nm using a PerkinElmer Victor2 plate reader (PerkinElmer, Shelton, CT).

X-ray Cocrystal Structure Determination of 3 in Complex with Aurora Kinase A. Cocrystal complex structure determination was carried out as reported in our previous publication using compound **3** as the inhibitor.[22]

X-ray Cocrystal Structure Determination of 8 in Complex with EGFR Kinase. (a) Expression and Purification of EGFR. EGFR catalytic domain (residues 696−1022) was cloned into the pBac-PAK8-MT-EGFP-GST vector and expressed in insect cells Hi5. The protein was purified by GST affinity column. The bound protein was washed with 1-fold PBS buffer solution and eluted with 20 mM GSH in 50 mM Tris-Cl (pH 8.0) buffer solution. The eluted fractions were then exchanged to PreScission digestion buffer (50 mM Tris-HCl, 150 mM NaCl, 1 mM EDTA, 1 mM DTT, pH 8.0) by desalting column, followed by treatment with PreScission protease (GE Healthcare) at 4 °C for 16 h to remove the GST tag, and then loaded to GST affinity column to recover follow-through. The follow-through was then buffer-exchanged and concentrated to 3−6 mg/mL in 20 mM Tris-Cl (pH 8.0), 5 mM DTT, 100 mM sodium chloride, and 0.5 mM EDTA buffer solution.

(b) Crystallization and structure determination. The hanging drop method was used to obtain crystals of the wild type EGFR catalytic domain. The crystals were grown at 18 °C for 1 week. Crystals of EGFR kinase complexed with compound were obtained by soaking apo-EGFR kinase crystals in reservoir solution containing 1.0 M ammonium citrate tribasic, pH 7.0, 0.1 M Bis-Tris propane, pH 7.0 (Hampton research), and 0.6 mM compound **8**. Before being flash-frozen in liquid nitrogen, the crystal was immersed briefly in a cryoprotectant containing 22.2% glycerol in soaking drop. Diffraction data were collected on beamlines BL13B1 (Taiwan). The data were processed by DENZO[23] and reduced with SCALEPACK. The structure was solved by molecular replacement in MOLREP[24] using the published EGFR structure (PDB ID 1M17) as the search model. The refinement calculations were performed by REFMAC5,[25] and model building was carried out with the program O11.[26]

Acknowledgment. We thank the staff of beamline BL13B1 at the National Synchrotron Radiation Research Centre (NSRRC), Taiwan, and SP12B2 at SPring-8, Japan, for technical assistance, as well as Chung-Yu Chang and Teng-Yuan Chang of the National Health Research Institutes for their assistance with Aurora and EGFR assay development. We also thank Mark Swofford for helping with the English editing. The authors acknowledge financial support by the National Science Council (Grant No. NSC-98-2119-M-400-001-MY3 to H-P.H.) and Department of Health (Grant No. DOH98-TD-G-111-019 to Y.-S.C. and Grant No. DOH98-TD-G-111-020 to H.-P.-H.), Taiwan, ROC.

Supporting Information Available: List of amines used for library synthesis, flow cytometry and Western blotting analysis for compound **3**, X-ray cocrystal structure of EGFR protein in complex with inhibitor **8**, X-ray refinement statistics for compounds **3** and **8**, and HPLC purity determination conditions. This material is available free of charge via the Internet at http://pubs.acs.org.

References

(1) Watkins, K. J. Fighting the clock. *Chem. Eng. News* **2002**, *80*, 27–33.
(2) Brik, A.; Wu, C. Y.; Wong, C. H. Microtiter plate based chemistry and in situ screening: a useful approach for rapid inhibitor discovery. *Org. Biomol. Chem.* **2006**, *4*, 1446–1457.

(3) Noble, M. E.; Endicott, J. A.; Johnson, L. N. Protein kinase inhibitors: insights into drug design from structure. *Science* **2004**, *303*, 1800–1805.
(4) Fu, J.; Bian, M.; Jiang, Q.; Zhang, C. Roles of Aurora kinases in mitosis and tumorigenesis. *Mol. Cancer Res.* **2007**, *5*, 1–10.
(5) Gautschi, O.; Heighway, J.; Mack, P. C.; Purnell, P. R.; Lara, P. N., Jr.; Gandara, D. R. Aurora kinases as anticancer drug targets. *Clin. Cancer Res.* **2008**, *14*, 1639–1648.
(6) Tiseo, M.; Loprevite, M.; Ardizzoni, A. Epidermal growth factor receptor inhibitors: a new prospective in the treatment of lung cancer. *Curr. Med. Chem.: Anti-Cancer Agents* **2004**, *4*, 139–148.
(7) Sharma, S. V.; Bell, D. W.; Settleman, J.; Haber, D. A. Epidermal growth factor receptor mutations in lung cancer. *Nat. Rev. Cancer* **2007**, *7*, 169–181.
(8) Coumar, M. S.; Tsai, M. T.; Chu, C. Y.; Uang, B. J.; Teng, C. H.; Chang, C. Y.; Chang, T. Y.; Lin, W. H.; Hsu, J. T. A.; Wu, J. S.; Wu, S. Y.; Chao, Y. S.; Hsieh, H. P. Identification, SAR studies and X-ray cocrystal analysis of a novel furano-pyrimidine Aurora kinase A inhibitor. *ChemMedChem* **2010**, *5*, 255–267.
(9) Foloppe, N.; Fisher, L. M.; Howes, R.; Kierstan, P.; Potter, A.; Robertson, A. G.; Surgenor, A. E. Structure-based design of novel Chk1 inhibitors: insights into hydrogen bonding and protein−ligand affinity. *J. Med. Chem.* **2005**, *48*, 4332–4345.
(10) Wu, C. Y.; Chang, C. F.; Chen, J. S.; Wong, C. H.; Lin, C. H. Rapid diversity-oriented synthesis in microtiter plates for in situ screening: discovery of potent and selective alpha-fucosidase inhibitors. *Angew. Chem., Int. Ed.* **2003**, *42*, 4661–4664.
(11) Lee, L. V.; Mitchell, M. L.; Huang, S. J.; Fokin, V. V.; Sharpless, K. B.; Wong, C. H. A potent and highly selective inhibitor of human alpha-1,3-fucosyltransferase via click chemistry. *J. Am. Chem. Soc.* **2003**, *125*, 9588–9589.
(12) Liao, J. J. Molecular recognition of protein kinase binding pockets for design of potent and selective kinase inhibitors. *J. Med. Chem.* **2007**, *50*, 409–424.
(13) Liu, Y.; Gray, N. S. Rational design of inhibitors that bind to inactive kinase conformations. *Nat. Chem. Biol.* **2006**, *2*, 358–364.
(14) Backes, A. C.; Zech, B.; Felber, B.; Klebl, B.; Muller, G. Small-molecule inhibitors binding to protein kinase. Part II: the novel pharmacophore approach of type II and type III inhibition. *Expert Opin. Drug Discovery* **2008**, *3*, 1427–1449.
(15) Harrington, E. A.; Bebbington, D.; Moore, J.; Rasmussen, R. K.; Ajose-Adeogun, A. O.; Nakayama, T.; Graham, J. A.; Demur, C.; Hercend, T.; Diu-Hercend, A.; Su, M.; Golec, J. M.; Miller, K. M. VX-680, a potent and selective small-molecule inhibitor of the Aurora kinases, suppresses tumor growth in vivo. *Nat. Med.* **2004**, *10*, 262–267.
(16) Wissner, A.; Mansour, T. S. The development of HKI-272 and related compounds for the treatment of cancer. *Arch. Pharm. (Weinheim, Ger.)* **2008**, *341*, 465–477.
(17) Fry, D. W.; Bridges, A. J.; Denny, W. A.; Doherty, A.; Greis, K. D.; Hicks, J. L.; Hook, K. E.; Keller, P. R.; Leopold, W. R.; Loo, J. A.; McNamara, D. J.; Nelson, J. M.; Sherwood, V.; Smaill, J. B.; Trumpp-Kallmeyer, S.; Dobrusin, E. M. Specific, irreversible inactivation of the epidermal growth factor receptor and erbB2, by a new class of tyrosine kinase inhibitor. *Proc. Natl. Acad. Sci. U.S.A.* **1998**, *95*, 12022–12027.
(18) Ciardiello, F.; Tortora, G. EGFR antagonists in cancer treatment. *N. Engl. J. Med.* **2008**, *358*, 1160–1174.
(19) Li, D.; Ambrogio, L.; Shimamura, T.; Kubo, S.; Takahashi, M.; Chirieac, L. R.; Padera, R. F.; Shapiro, G. I.; Baum, A.; Himmelsbach, F.; Rettig, W. J.; Meyerson, M.; Solca, F.; Greulich, H.; Wong, K. K. BIBW2992, an irreversible EGFR/HER2 inhibitor highly effective in preclinical lung cancer models. *Oncogene* **2008**, *27*, 4702–4711.
(20) Coumar, M. S.; Wu, J. S.; Leou, J. S.; Tan, U. K.; Chang, C. Y.; Chang, T. Y.; Lin, W. H.; Hsu, J. T.; Chao, Y. S.; Wu, S. Y.; Hsieh, H. P. Aurora kinase A inhibitors: identification, SAR exploration and molecular modeling of 6,7-dihydro-4*H*-pyrazolo-[1,5-*a*]-pyrrolo[3,4-d]pyrimidine-5,8-dione scaffold. *Bioorg. Med. Chem. Lett.* **2008**, *18*, 1623–1627.
(21) Lin, W. H.; Song, J. S.; Chang, T. Y.; Chang, C. Y.; Fu, Y. N.; Yeh, C. L.; Wu, S. H.; Huang, Y. W.; Fang, M. Y.; Lien, T. W.; Hsieh, H. P.; Chao, Y. S.; Huang, S. F.; Tsai, S. F.; Wang, L. M.; Hsu, J. T.; Chen, Y. R. A cell-based high-throughput screen for epidermal growth factor receptor pathway inhibitors. *Anal. Biochem.* **2008**, *377*, 89–94.
(22) Coumar, M. S.; Leou, J. S.; Shukla, P.; Wu, J. S.; Dixit, A. K.; Lin, W. H.; Chang, C. Y.; Lien, T. W.; Tan, U. K.; Chen, C. H.; Hsu, J. T.; Chao, Y. S.; Wu, S. Y.; Hsieh, H. P. Structure-based drug design of novel Aurora kinase A inhibitors: structural basis for potency and specificity. *J. Med. Chem.* **2009**, *52*, 1050–1062.
(23) Otwinowski, Z.; Minor, W. Processing of x-ray diffraction data collected in oscillation mode. *Methods Enzymol.* **1997**, *276*, 307–326.
(24) Vagin, A; Teplyakov, A. MOLREP: an automated program for molecular replacement. *J. Appl. Crystallogr.* **1997**, *30*, 1022–1025.
(25) Murshudov, G. N.; Vagin, A. A.; Dodson, E. J. Refinement of macromolecular structures by the maximum-likelihood method. *Acta Crystallogr.* **1997**, *D53*, 240–255.
(26) Jones, T. A.; Zou, J.-Y.; Cowan, S. W.; Kjeldgaard Improved methods for building protein models in electron density maps and the location of errors in these models. *Acta Crystallogr.* **1991**, *A47*, 110–119.